

Supramolecular polymer-directed light-harvesting system based on a stepwise energy transfer cascade

Tangxin Xiao,* Liangliang Zhang, Haoran Wu, Hongwei Qian, Dongxing Ren, Zheng-Yi Li and Xiao-Qiang Sun

Jiangsu Key Laboratory of Advanced Catalytic Materials and Technology, School of Petrochemical Engineering, Changzhou University, Changzhou, 213164, China.

E-mail: xiaotangxin@cczu.edu.cn

Table of contents

1. Materials, methods, and abbreviations.....	S2
2. AIE and SAIE behaviors of M	S4
3. Fluorescence lifetime measurements.....	S4
4. Quantum yield measurements.....	S5
5. Energy-transfer efficiency calculation.....	S6
6. Antenna effect calculation.....	S9
7. Control experiment of NDI@M for light-harvesting.....	S13
8. White-light emission.....	S13
9. Fluorescence images of supramolecular nanoparticles.....	S14
10. References.....	S15

1. Materials, methods, and abbreviations

General

All chemicals, reagents and solvents were purchased from commercial suppliers and used, unless otherwise stated, without further purification. If needed, solvents were dried by literature known procedures. **M** was synthesized according to our recent report.^[S1] **NDI** was synthesized according to literature.^[S2]

NMR spectroscopy

The ¹H NMR and ¹³C NMR spectra were recorded with a Bruker AVANCE III (300 MHz) spectrometer and calibrated against the residual proton signal or natural abundance carbon resonance of the used deuterated solvent from tetramethylsilane (TMS) as the internal standard. The chemical shifts δ are indicated in ppm and the coupling constants J in Hz. The multiplicities are given as s (singlet), d (doublet), dd (doublet of doublets), t (triplet), and m (multiplet).

Transmission electron microscope (TEM)

TEM investigations were carried out on a JEM-2100 instrument.

Dynamic light scattering (DLS)

DLS measurements were carried out on a Brookhaven BI-9000AT system, equipped with a 200 mW polarized laser source ($\lambda = 514$ nm) at a scattering angle of 90°. All samples were prepared according to the corresponding procedures mentioned above.

UV-Vis spectroscopy

The UV-Vis absorption spectra were measured on a Perkin Elmer Lambda 35 UV-Vis Spectrometer.

Fluorescence spectroscopy

Fluorescence measurements were performed on an Agilent Cary Eclipse spectrofluorometer.

Fluorescence lifetimes

The fluorescence lifetimes were measured employing time correlated single photon counting on a FLS980 instrument with a pulsed xenon lamp. Analysis of fluorescence decay curves were subjected

to fit a mono-exponential or bi-exponential decay. The instrument response function (IRF) measures the scattering of laser excitation from non-fluorescent control samples to determine the fastest possible response of the detectors.

Quantum yields

The quantum yields were carried out on a FLS980 instrument with the integrating sphere.

CIE coordinates

The CIE (Commission Internationale de l'Eclairage) 1931 coordinates were calculated with the method of color matching functions.

Abbreviations

THF = Tetrahydrofuran; NPs = nanoparticles; DCM = dichloromethane

M = mol/L; br = broad; Ar = aromatic group

2. AIE and SAIE behaviors of M

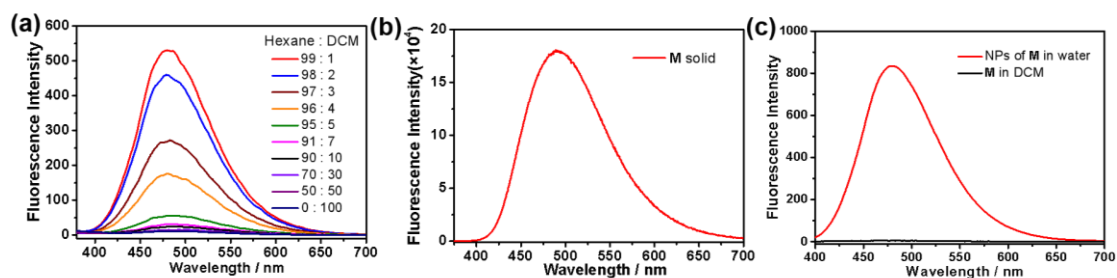


Fig. S1. (a) Fluorescence spectra of **M** in mixed DCM/hexane solution at different vol% upon excitation at 330 nm, $[M] = 5 \times 10^{-5}$ M, (b) solid-state fluorescence spectrum of **M**, (c) fluorescence spectra of molecule **M** in DCM and NPs of **M** in water upon excitation at 330 nm, $[M] = 5 \times 10^{-5}$ M.

3. Fluorescence lifetime measurements

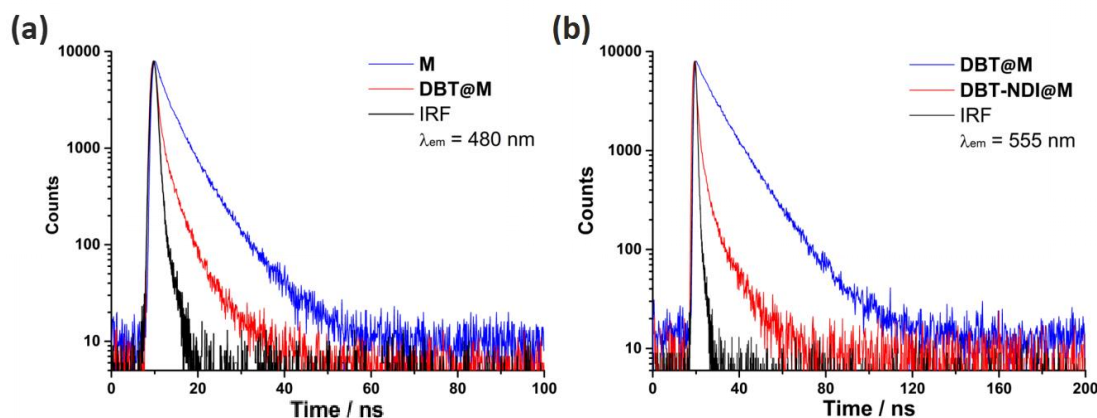


Fig. S2. Fluorescence decay profiles of (a) **M** NPs and **DBT@M** NPs monitored at 480 nm upon excitation at 365 nm and (b) **DBT@M** NPs and **DBT-NDI@M** monitored at 555 nm upon excitation at 365 nm in aqueous solution. $[M] = 5 \times 10^{-5}$ M, $[DBT] = 1 \times 10^{-6}$ M, $[NDI] = 5 \times 10^{-7}$ M, respectively.

Table S1. Fluorescence lifetimes of **M** NPs and **DBT@M** NPs monitored at 480 nm upon excitation at 365 nm in aqueous solution, $[M] = 5 \times 10^{-5}$ M, $[DBT] = 1 \times 10^{-6}$ M, respectively.

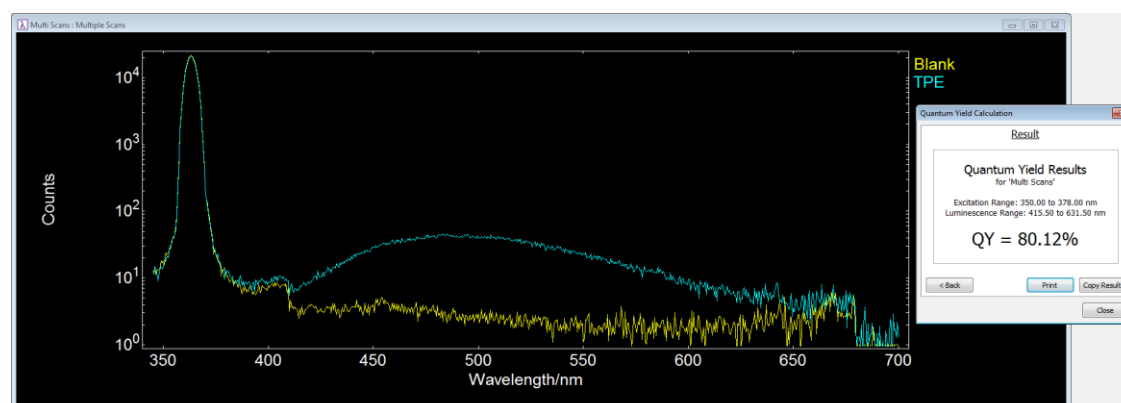
Sample	τ_1/ns	RW1[%]	τ_2/ns	RW2[%]	τ/ns	χ^2
M	3.67	36.7	8.14	63.3	6.50	1.060
DBT@M (M : DBT = 50 : 1)	0.86	25.0	3.44	75.0	2.80	0.981

Table S2. Fluorescence lifetimes of **DBT@M** NPs and **DBT-NDI@M** NPs monitored at 555 nm upon excitation at 365 nm in aqueous solution, $[M] = 5 \times 10^{-5}$ M, $[DBT] = 1 \times 10^{-6}$ M, $[NDI] = 5 \times 10^{-7}$ M, respectively.

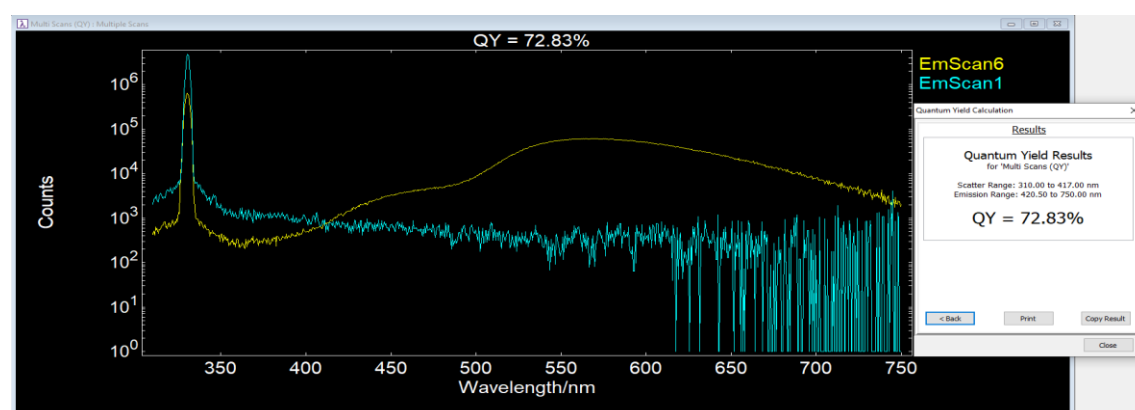
Sample	τ_1/ns	RW1[%]	τ_2/ns	RW2[%]	τ/ns	χ^2
DBT@M	5.50	18.89	13.95	85.38	12.72	0.982
DBT-NDI@M (M : DBT : NDI = 2500 : 50 : 25)	1.65	47.3	8.72	52.7	5.37	1.099

4. Quantum yield measurements

(a)



(b)



(c)

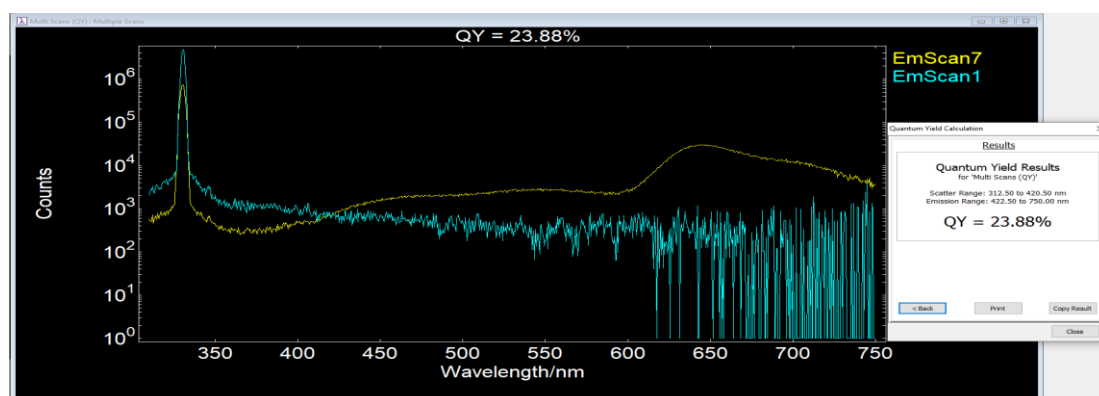


Fig. S3. Absolute fluorescence quantum yields ($\Phi_{f(\text{abs})}$) of (a) **M** NPs, (b) **DBT@M** NPs, and (c) **DBT-NDI@M** NPs upon excitation at 330 nm in aqueous solution, $[\text{M}] = 5 \times 10^{-5}$ M, $[\text{DBT}] = 1 \times 10^{-6}$ M, $[\text{NDI}] = 5 \times 10^{-7}$ M, respectively.

Table S3. Fluorescence quantum yields of NPs of **M**, **DBT@M**, **DBT-NDI@M**, $[\text{M}] = 5 \times 10^{-5}$ M, $[\text{DBT}] = 1 \times 10^{-6}$ M, $[\text{NDI}] = 5 \times 10^{-7}$ M, respectively.

Sample	Fluorescence quantum yields ($\Phi_{f(\text{abs})}$)
M	80.12%
DBT@M (M : DBT = 50 : 1)	72.83%
DBT-NDI@M (M : DBT : NDI = 2500 : 50 : 25)	23.88%

5 Energy-transfer efficiency calculation

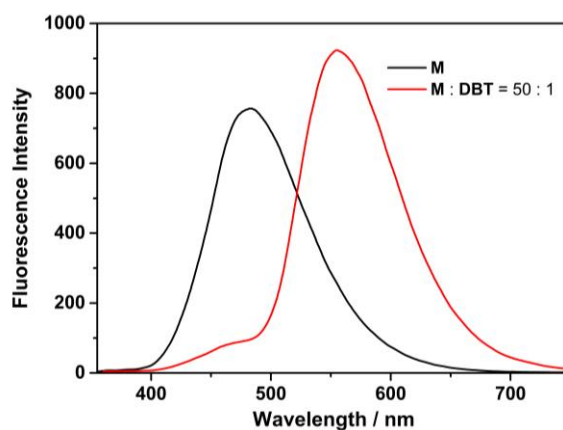


Fig. S4. Fluorescence spectrum of **M** and **DBT@M**. $[\text{M}] = 5 \times 10^{-5}$ M, $[\text{DBT}] = 1 \times 10^{-6}$ M, respectively.

Energy-transfer efficiency (Φ_{ET}) was calculated from fluorescence spectra by the equation S1^[S3]:

$$\Phi_{ET} = 1 - I_{DA} / I_D \text{ (eq. S1)}$$

Where I_{DA} and I_D are the fluorescence intensities of the donor (**M**) at 480 nm in the presence (Fig. S3, red line) and absence (Fig. S3, black line) of the acceptor (**DBT**), respectively, when excited at 330 nm.

The Φ_{ET} was calculated to be 87.4% under the condition of $[M] = 5 \times 10^{-5}$ M and $[DBT] = 1 \times 10^{-6}$ M ($\lambda_{ex} = 330$ nm and $\lambda_{em} = 480$ nm).

Similarly, the Φ_{ET} of other **M/DBT** ratios could also be calculated according to this equation.

Table S4. Energy-transfer efficiency with different **M/DBT** ratio.

Sample	Concentration, respectively	Energy-transfer efficiency (Φ_{ET})
DBT@M (M : DBT = 50 : 1)	$[M] = 5 \times 10^{-5}$ M $[DBT] = 1 \times 10^{-6}$ M	87.4%
DBT@M (M : DBT = 75 : 1)	$[M] = 5 \times 10^{-5}$ M $[DBT] = 6.66 \times 10^{-7}$ M	79.4%
DBT@M (M : DBT = 100 : 1)	$[M] = 5 \times 10^{-5}$ M $[DBT] = 5 \times 10^{-7}$ M	69.0%
DBT@M (M : DBT = 125 : 1)	$[M] = 5 \times 10^{-5}$ M $[DBT] = 4 \times 10^{-7}$ M	60.0%
DBT@M (M : DBT = 166 : 1)	$[M] = 5 \times 10^{-5}$ M $[DBT] = 3 \times 10^{-7}$ M	56.5%
DBT@M (M : DBT = 200 : 1)	$[M] = 5 \times 10^{-5}$ M $[DBT] = 2.5 \times 10^{-7}$ M	49.2%
DBT@M (M : DBT = 250 : 1)	$[M] = 5 \times 10^{-5}$ M $[DBT] = 2 \times 10^{-7}$ M	43.8%
DBT@M (M : DBT = 300 : 1)	$[M] = 5 \times 10^{-5}$ M $[DBT] = 1.67 \times 10^{-7}$ M	39.5%
DBT@M (M : DBT = 400 : 1)	$[M] = 5 \times 10^{-5}$ M $[DBT] = 1.25 \times 10^{-7}$ M	31.7%
DBT@M (M : DBT = 750 : 1)	$[M] = 5 \times 10^{-5}$ M $[DBT] = 6.67 \times 10^{-8}$ M	26.7%

DBT@M (M : DBT = 1000 : 1)	[M] = 5×10^{-5} M [DBT] = 5×10^{-8} M	21.6%
DBT@M (M : DBT = 3000 : 1)	[M] = 5×10^{-5} M [DBT] = 1.67×10^{-8} M	15.8%

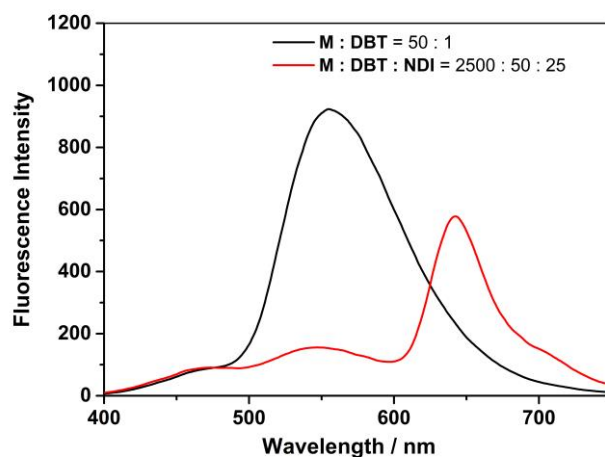


Fig. S5. Fluorescence spectra of **DBT@M** and **DBT-NDI@M**, **[M]** = 5×10^{-5} M, **[DBT]** = 1×10^{-6} M, **[NDI]** = 5×10^{-7} M, respectively.

The Φ_{ET} of the second-step FRET was also calculated by the equation S1^[S3]:

$$\Phi_{ET} = 1 - I_{DA} / I_D \text{ (eq. S1)}$$

At this moment, **DBT** (relay acceptor) plays the role of donor and **NDI** acts as acceptor. Herein, I_{DA} and I_D are the fluorescence intensities of the emission of **DBT** at 555 nm in **DBT-NDI@M** NPs (Fig. S4, red line) and **DBT@M** NPs (Fig. S4, black line), respectively, when excited at 330 nm.

The Φ_{ET} was calculated as 83.4% in water, measured under the condition of **[M]** = 5×10^{-5} M, **[DBT]** = 1×10^{-6} M, **[NDI]** = 5×10^{-7} M, λ_{ex} = 330 nm.

Similarly, the Φ_{ET} of other **M/DBT/NDI** ratios could also be calculated using this method.

Table S5. Energy-transfer efficiency with different **M/DBT/NDI** ratio.

Sample	Concentration, respectively	Energy-transfer efficiency (Φ_{ET})
DBT-NDI@M (M : DBT : NDI = 2500 : 50 : 25)	[M] = 5×10^{-5} M [DBT] = 1×10^{-6} M [NDI] = 5×10^{-7} M	83.4%
DBT-NDI@M (M : DBT : NDI = 2500 : 50 : 10)	[M] = 5×10^{-5} M [DBT] = 1×10^{-6} M [NDI] = 2×10^{-7} M	77.3%
DBT-NDI@M (M : DBT : NDI = 2500 : 50 : 5)	[M] = 5×10^{-5} M [DBT] = 1×10^{-6} M [NDI] = 1×10^{-7} M	57.4%
DBT-NDI@M (M : DBT : NDI = 2500 : 50 : 2)	[M] = 5×10^{-5} M [DBT] = 1×10^{-6} M [NDI] = 4×10^{-8} M	39.4%
DBT-NDI@M (M : DBT : NDI = 2500 : 50 : 1)	[M] = 5×10^{-5} M [DBT] = 1×10^{-6} M [NDI] = 2×10^{-8} M	25.7%

6 Antenna effect calculation

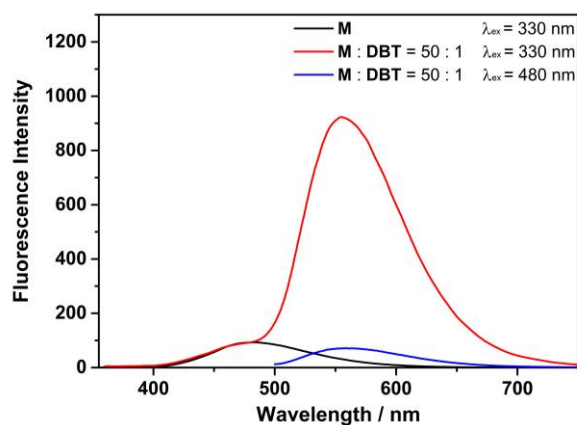


Fig. S6. Fluorescence spectra of **DBT@M** (red line: $\lambda_{ex} = 330$ nm; blue line: $\lambda_{ex} = 480$ nm). The black line represents the fluorescence spectrum of **M**, which was normalized according to the fluorescence intensity at 480 nm of the red line. [**M**] = 5×10^{-5} M, [**DBT**] = 1×10^{-6} M, respectively.

The antenna effect (AE) was calculated according to equation S2^[S3]:

$$AE = (I_{DA,330} - I_{D,330}) / I_{DA,480} \text{ (eq. S2)}$$

Where $I_{DA,330}$ is the fluorescence intensity of **DBT** at 555 nm with the excitation of the donor at 330 nm (Fig. S5, red line). $I_{DA,480}$ is the fluorescence intensity of **DBT** at 555 nm with the direct excitation of the acceptor at 480 nm (Fig. S5, blue line). $I_{D,330}$ is the normalized fluorescence intensity of individual **M** at 555 nm.

The AE value was calculated as 12.6 under the condition of $[M] = 5 \times 10^{-5}$ M, $[DBT] = 1 \times 10^{-6}$ M, respectively.

Similarly, the antenna effect of other **M/DBT** ratios was also calculated according to this equation.

Table S6. Antenna effect with different **M/DBT** ratio.

Sample	Concentration, respectively	Antenna effect (AE)
DBT@M (M : DBT = 50 : 1)	$[M] = 5 \times 10^{-5}$ M $[DBT] = 1 \times 10^{-6}$ M	12.6
DBT@M (M : DBT = 75 : 1)	$[M] = 5 \times 10^{-5}$ M $[DBT] = 6.66 \times 10^{-7}$ M	18.2
DBT@M (M : DBT = 100 : 1)	$[M] = 5 \times 10^{-5}$ M $[DBT] = 5 \times 10^{-7}$ M	22.2
DBT@M (M : DBT = 125 : 1)	$[M] = 5 \times 10^{-5}$ M $[DBT] = 4 \times 10^{-7}$ M	23.9
DBT@M (M : DBT = 166 : 1)	$[M] = 5 \times 10^{-5}$ M $[DBT] = 3 \times 10^{-7}$ M	25.8
DBT@M (M : DBT = 200 : 1)	$[M] = 5 \times 10^{-5}$ M $[DBT] = 2.5 \times 10^{-7}$ M	26.7
DBT@M (M : DBT = 250 : 1)	$[M] = 5 \times 10^{-5}$ M $[DBT] = 2 \times 10^{-7}$ M	27.6
DBT@M (M : DBT = 300 : 1)	$[M] = 5 \times 10^{-5}$ M $[DBT] = 1.67 \times 10^{-7}$ M	27.8
DBT@M (M : DBT = 400 : 1)	$[M] = 5 \times 10^{-5}$ M $[DBT] = 1.25 \times 10^{-7}$ M	27.3
DBT@M (M : DBT = 750 : 1)	$[M] = 5 \times 10^{-5}$ M $[DBT] = 6.67 \times 10^{-8}$ M	26.6
DBT@M (M : DBT = 1000 : 1)	$[M] = 5 \times 10^{-5}$ M $[DBT] = 5 \times 10^{-8}$ M	23.5

DBT@M (**M** : **DBT** = 3000 : 1)

$[\mathbf{M}] = 5 \times 10^{-5} \text{ M}$
 $[\mathbf{DBT}] = 1.67 \times 10^{-8} \text{ M}$

16.2

Generally, the antenna effect (AE) should increase upon the decrease of acceptor. However, the AE first increases and then decreases upon the decrease of acceptor in this case. It might be because the fluorescence intensity of **DBT@M** excited at 480 nm (the blue line, Fig. S6, ESI†) is very approaching to the base line (blank sample) at relative high D/A ratio and doesn't change much upon the further decrease of acceptor. But at the same time, the fluorescence intensity of **DBT@M** excited at 330 nm (the red line, Fig. S6, ESI†) continues to decrease, eventually resulting in a decrease of the AE upon the further decrease of acceptor. Notably, $AE = (I_{DA,330} - I_{D,330}) / I_{DA,480}$. Intuitively, the AE is proportional to $I_{\text{red line}}/I_{\text{blue line}}$ (Fig. S6, ESI†). Similar phenomena could be also found in other reported examples (see Figure 2 in *Angew. Chem. Int. Ed.* **2020**, *59*, 10493-10497).

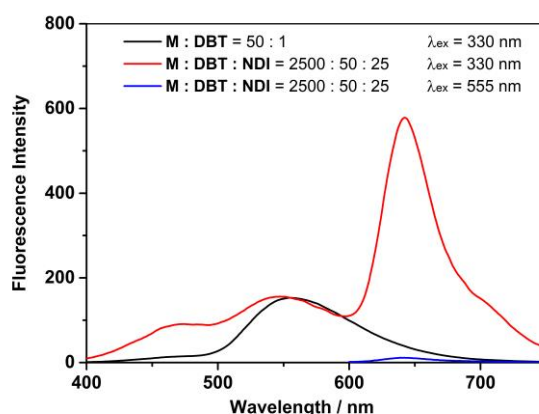


Fig. S7. Fluorescence spectra of **DBT-NDI@M** (red line: $\lambda_{\text{ex}} = 330 \text{ nm}$; blue line: $\lambda_{\text{ex}} = 555 \text{ nm}$). The black line represents the fluorescence spectrum of **DBT@M**, which was normalized according to the fluorescence intensity at 555 nm of the red line. $[\mathbf{M}] = 5 \times 10^{-5} \text{ M}$, $[\mathbf{DBT}] = 1 \times 10^{-6} \text{ M}$, $[\mathbf{NDI}] = 5 \times 10^{-7} \text{ M}$, respectively.

The AE was also calculated based on the emission spectra using equation S2^[S3]:

$$AE = (I_{DA,330} - I_{D,330}) / I_{DA,555} \text{ (eq. S2)}$$

At this moment, **DBT** (relay acceptor) plays the role of donor and **NDI** acts as acceptor. Herein, $I_{DA,330}$ and $I_{DA,555}$ are the **NDI** fluorescence intensity at 640 nm with the excitation of the donor at

330 nm and the direct excitation of the acceptor at 555 nm, respectively. $I_{D,330}$ is the fluorescence intensities at 640 nm of the **DBT@M** NPs, which was normalized with the **DBT-NDI@M** NPs at 555 nm.

The AE value was calculated to be 47.6 under the condition of $[M] = 5 \times 10^{-5}$ M, $[DBT] = 1 \times 10^{-6}$ M, $[NDI] = 5 \times 10^{-7}$ M, respectively.

Similarly, the antenna effect of other **M/DBT/NDI** ratios could also be calculated according to this equation.

Table S7. Antenna effect with different **M/DBT/NDI** ratio.

Sample	Concentration, respectively	Antenna effect (AE)
DBT-NDI@M (M : DBT : NDI = 2500 : 50 : 25)	$[M] = 5 \times 10^{-5}$ M $[DBT] = 1 \times 10^{-6}$ M $[NDI] = 5 \times 10^{-7}$ M	47.6
DBT-NDI@M (M : DBT : NDI = 2500 : 50 : 10)	$[M] = 5 \times 10^{-5}$ M $[DBT] = 1 \times 10^{-6}$ M $[NDI] = 2 \times 10^{-7}$ M	51.3
DBT-NDI@M (M : DBT : NDI = 2500 : 50 : 5)	$[M] = 5 \times 10^{-5}$ M $[DBT] = 1 \times 10^{-6}$ M $[NDI] = 1 \times 10^{-7}$ M	55.9
DBT-NDI@M (M : DBT : NDI = 2500 : 50 : 2)	$[M] = 5 \times 10^{-5}$ M $[DBT] = 1 \times 10^{-6}$ M $[NDI] = 4 \times 10^{-8}$ M	63.1
DBT-NDI@M (M : DBT : NDI = 2500 : 50 : 1)	$[M] = 5 \times 10^{-5}$ M $[DBT] = 1 \times 10^{-6}$ M $[NDI] = 2 \times 10^{-8}$ M	56.2

7 Control experiment of NDI@M for light-harvesting

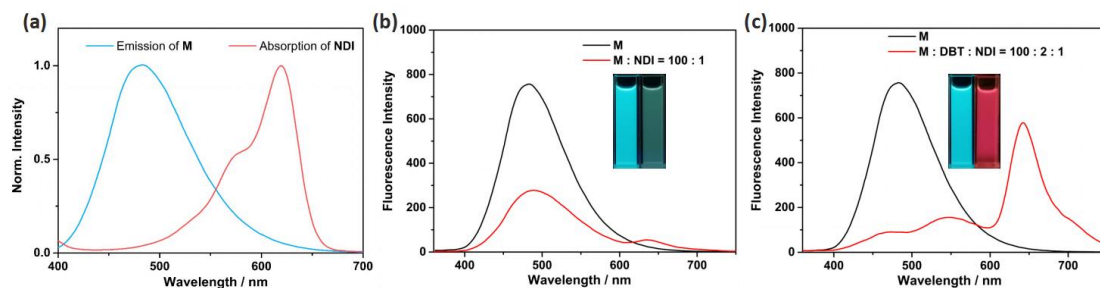


Fig. S8. (a) Normalized fluorescence spectra of **M** (blue line) and normalized absorbance spectra of **NDI** (red line). (b) Fluorescence spectra of **M** and **NDI@M** upon excitation at 330 nm. Inset: Photographs of NPS of **M** and **M@NDI**, $[M] = 5 \times 10^{-5}$ M, $[NDI] = 5 \times 10^{-7}$ M, respectively. (c) Fluorescence spectra of **M** and **DBT@NDI@M** upon excitation at 330 nm. Inset: Photographs of NPS of **M** and **DBT@NDI@M**, $[M] = 5 \times 10^{-5}$ M, $[DBT] = 1 \times 10^{-6}$ M, $[NDI] = 5 \times 10^{-7}$ M, respectively.

8 White-light emission

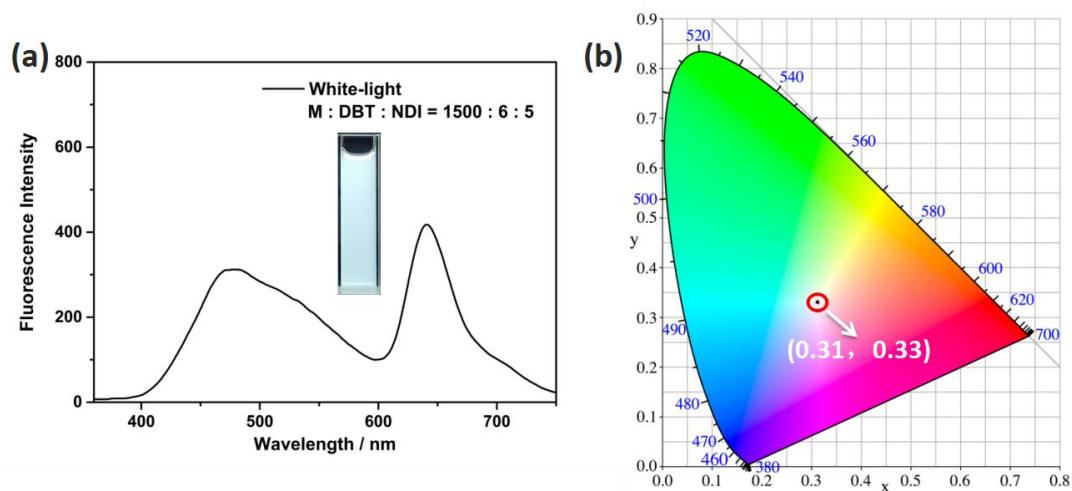


Fig. S9. (a) Fluorescence spectrum of the white-light emitting coordinate. Inset: fluorescent image of the corresponding solution, $[M] = 5 \times 10^{-5}$ M, $[DBT] = 2 \times 10^{-7}$ M, $[NDI] = 1.67 \times 10^{-7}$ M. (b) The CIE chromaticity diagram of the white-light emitting coordinate (0.31, 0.33).

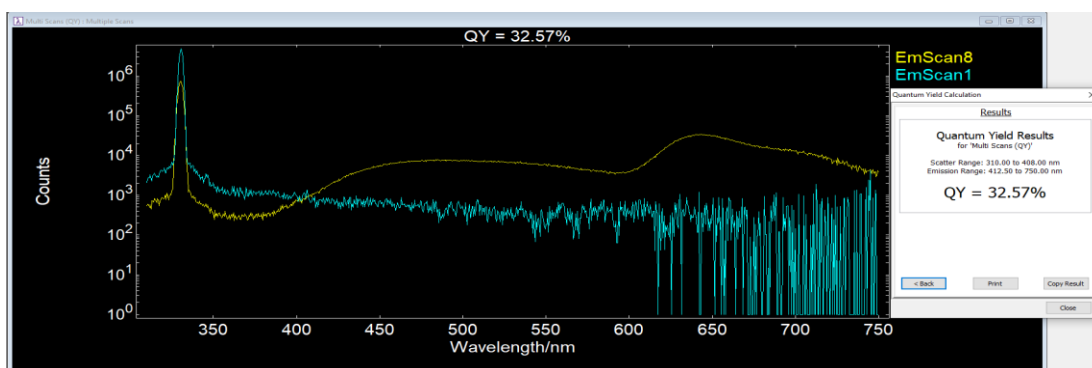


Fig. S10. Absolute fluorescence quantum yields ($\Phi_{f(\text{abs})}$) of **DBT-NDI@M** (white-light emitting) NPs upon excitation at 330 nm in aqueous solution, $[\mathbf{M}] = 5 \times 10^{-5}$ M, $[\mathbf{DBT}] = 2 \times 10^{-7}$ M, $[\mathbf{NDI}] = 1.67 \times 10^{-7}$ M.

Table S8. Fluorescence quantum yields of **DBT-NDI@M** (white-light emitting), $[\mathbf{M}] = 5 \times 10^{-5}$ M, $[\mathbf{DBT}] = 2 \times 10^{-7}$ M, $[\mathbf{NDI}] = 1.67 \times 10^{-7}$ M.

Sample	Fluorescence quantum yields
	($\Phi_{f(\text{abs})}$)
DBT-NDI@M (M : DBT : NDI = 1500 : 6 : 5)	32.57%

9 Fluorescence images of supramolecular nanoparticles

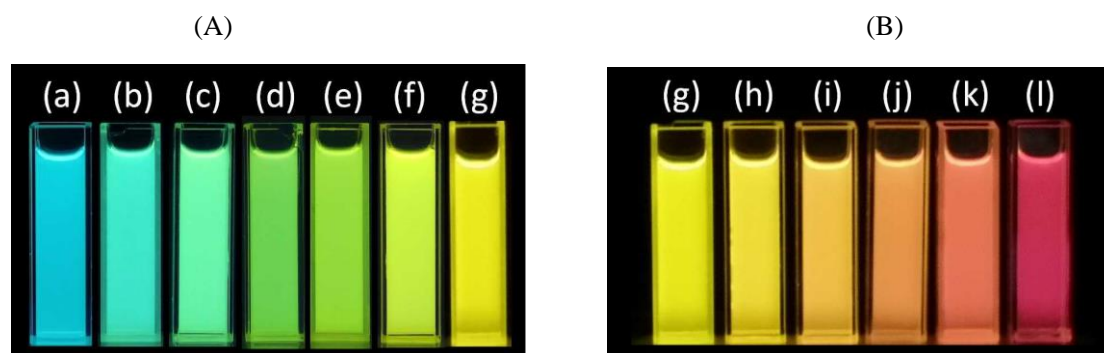


Fig. S11. Fluorescence images: (A) The first energy transfer of **M** (5×10^{-5} M) with different concentration of **DBT**: (a) 0 M, (b) 5×10^{-8} M, (c) 1.25×10^{-7} M, (d) 2.0×10^{-7} M, (e) 4×10^{-7} M, (f) 5×10^{-7} M, and (g) 1×10^{-6} M, respectively. (B) The sequential energy transfer of **M** (5×10^{-5} M) and **DBT** (1×10^{-6} M) with different concentration of **NDI**: (g) 0 M, (h) 2×10^{-8} M, (i) 4×10^{-8} M, (j) 1×10^{-7} M, (k) 2×10^{-7} M, (l) 5×10^{-7} M.

10 References

- [S1] T. Xiao, H. Wu, G. Sun, K. Diao, X. Wei, Z. Y. Li, X. Q. Sun and L. Wang, An efficient artificial light-harvesting system with tunable emission in water constructed from a H-bonded AIE supramolecular polymer and Nile Red, *Chem. Commun.*, 2020, **56**, 12021-12024.
- [S2] Y. V. Suseela, M. Sasikumar and T. Govindaraju, An effective and regioselective bromination of 1,4,5,8-naphthalenetetracarboxylic dianhydride using tribromoisocyanuric acid, *Tetrahedron Lett.*, 2013, **54**, 6314-6318.
- [S3] M. Hao, G. Sun, M. Zuo, Z. Xu, Y. Chen, X. Y. Hu and L. Wang, A supramolecular artificial light-harvesting system with two-step sequential energy transfer for photochemical catalysis, *Angew. Chem. Int. Ed.*, 2020, **59**, 10095-10100.